Climatic Change (2006) 79:213–241
DOI 10.1007/s10584-006-9113-7

Arctic climate change with a 2 °C global warming: Timing, climate patterns and vegetation change

Jed O. Kaplan · Mark New

Received: 22 February 2005 / Accepted: 15 December 2005 / Published online: 20 October 2006

Abstract The signatories to United Nations Framework Convention on Climate Change are charged with stabilizing the concentrations of greenhouse gases in the atmosphere at a level that prevents dangerous interference with the climate system. A number of nations, organizations and scientists have suggested that global mean temperature should not rise over 2 °C above preindustrial levels. However, even a relatively moderate target of 2 °C has serious implications for the Arctic, where temperatures are predicted to increase at least 1.5 to 2 times as fast as global temperatures. High latitude vegetation plays a significant role in the lives of humans and animals, and in the global energy balance and carbon budget. These ecosystems are expected to be among the most strongly impacted by climate change over the next century. To investigate the potential impact of stabilization of global temperature at 2 °C, we performed a study using data from six Global Climate Models (GCMs) forced by four greenhouse gas emissions scenarios, the BIOME4 biogeochemistry-biogeography model, and remote sensing data. GCM data were used to predict the timing and patterns of Arctic climate change under a global mean warming of 2 °C. A unified circumpolar classification recognizing five types of tundra and six forest biomes was used to develop a map of observed Arctic vegetation. BIOME4 was used to simulate the vegetation distributions over the Arctic at the present and for a range of 2 °C global warming scenarios. The GCMs simulations indicate that the earth will have warmed by 2 °C relative to preindustrial temperatures by between 2026 and 2060, by which stage the area-mean annual temperature over the Arctic (60–90°N) will have increased by between 3.2 and 6.6 °C. Forest extent is predicted by BIOME4 to increase in the Arctic on the order of 3×10^6 km^2 or 55% with a corresponding 42% reduction in tundra area. Tundra types generally also shift north with the largest reductions in

Both authors contributed equally to the research and writing of the article.

J. O. Kaplan (✉)
Institute of Plant Sciences, University of Bern, Altenbergrain 21, 3013 Bern, Switzerland
e-mail: jed.kaplan@ips.unibe.ch

M. New
Climate Research Lab, Centre for the Environment, Oxford University, South Parks Road, Oxford OX1 3QY, England
e-mail: mark.new@ouce.ox.ac.uk

the prostrate dwarf-shrub tundra, where nearly 60% of habitat is lost. Modeled shifts in the potential northern limit of trees reach up to 400 km from the present tree line, which may be limited by migration rates. Simulated physiological effects of the CO_2 increase (to ca. 475 ppm) at high latitudes were small compared with the effects of the change in climate. The increase in forest area of the Arctic could sequester 600 Pg of additional carbon, though this effect is unlikely to be realized over next century.

1 Introduction

The goal of the United Nations Framework Convention on Climate Change is to stabilize the concentration of greenhouse gases in the atmosphere at a level that would prevent "dangerous anthropogenic interference with the climate system". Agreement on the level of warming that can be called dangerous remains a crucial task for policymakers. Several governments, the European Union, a number of environmental NGOs, and some scientists (for example, Hansen 2005) consider a global mean warming of 2 °C above preindustrial temperature to be a preliminary target. However, stabilization at a given global mean temperature change does not mean that the same changes will be experienced in different regions, as the spatial patterns of climate change will be very different to the global mean changes (IPCC 2001b, Figures 9.10 and 9.11).

One of the most striking results from transient global climate model (GCM) simulations of the effect of increased levels of greenhouse gases (GHGs) on the Earth's climate is the latitudinal variation in the amount of warming, with the greatest warming in the Arctic (Flato and Boer 2001; IPCC 2001b; Holland and Bitz 2003; Flato 2004; Hu et al. 2004). Most GCMs predict temperature changes at least twice the global mean temperature change for a doubling of atmospheric CO_2 concentrations over preindustrial levels. Thus even a moderate global temperature stabilization target such as 2 °C will have substantial implications for the Arctic.

Reasons for the enhanced warming over the Arctic are fairly well-understood, and have been reviewed by several authors (IPCC 2001b; Holland and Bitz 2003; Flato 2004; Hu et al. 2004; New 2005). The main drivers in GCMs are the ice/snow albedo effect, cloud cover and ocean circulation changes. These are all reinforced by the strong static stability of the lower troposphere (the Arctic inversion), which tends to focus any additional heating near the surface.

The snow/ice albedo effect occurs because reductions in snow, land ice and sea ice reduce reflectivity, permitting more incoming radiation to be absorbed and heat the ground and ocean; thinner sea-ice and ice-free water also result in larger heat fluxes to the atmosphere from the warmer ocean, with this effect being especially strong in spring and autumn. Sea ice changes dominate the ice/snow feedback in spring, summer and autumn, but reduction in snow cover and permafrost can have important regional effects over continental areas. The effect of snow cover is complicated by the interactions of increasing precipitation (which, if acting alone, would also mean more snowfall) and warming (which leads to faster snowmelt and rainfall being greater fraction of total precipitation).

Clouds act to both reduce incoming shortwave radiation through reflection and increase longwave flux back to the surface (Ingram et al. 1989). The net effect of these competing processes currently produces a positive (warming) forcing in winter and negative forcing for a several weeks in summer, with an overall net positive forcing (Curry et al. 1996). The sign of any cloud feedback in GCM simulations is therefore critically dependent on predicted changes in seasonal cloud cover. Holland and Bitz (2003) suggest that, in the

majority of GCMs for which cloud cover data were available in the CMIP2 study, ice-albedo changes dominate any negative cloud feedbacks, while increases in higher altitude cloud cover produces an additional (but small) positive feedback.

Poleward ocean heat transport can play a direct and indirect role in Arctic temperature change. Alterations in the strength and/or location of heat transport will directly affect the amount of warming, and also indirectly affect the ice-albedo feedback by influencing the nature of sea-ice retreat (Holland and Bitz 2003). Compared to their control climates, most current GCMs show a reduction in northward ocean heat transport in the North Atlantic ($<65°$N), which is correlated with a reduced rate of warming in this sector. At higher latitudes ($>65°$N), most GCMs show increased poleward ocean heat transport. The heat source and mechanism for this high latitude transport is unclear, given the reduced transport through the North Atlantic. Suggestions include atmospheric heat transport and then exchange with the ocean at higher latitudes (Holland and Bitz 2003), a simple export from the northern North Atlantic, which contributes to the overall reduced rate of warming in this sector, and/or transport of locally warmed water at the areas of greatest ice loss. Increased heat transport north of 65°N is correlated with a decrease in ice thickness and ice extent, and may also be an amplifying factor in these sea-ice changes (Holland and Bitz 2003).

Records of temperature change over the 20th century show similar Arctic temperature "amplification" relative to the global mean change, at least for the latter third of the century (Jones et al. 1999; Serreze et al. 2000; Johannessen et al. 2004), though the location of greatest warming differs between GCMs and observations,[1] and is not unanimously attributed to a high-latitude amplification of a GHG signal (Przybylak 2000; Polyakov et al. 2002; Polyakov et al. 2003). Part of the disagreement between authors is due to the periods over which the analysis takes place, as the Arctic has relatively large low-frequency (10–50 year) variability; recent observed warming, while consistent with GCM simulations, is not inconsistent with estimates of low frequency variability.

The natural vegetation of the Arctic is a keystone in the culture of its indigenous peoples and is essential to the survival of flagship animal species. The Arctic has a unique and rich flora and fauna that includes many endemics (ACIA 2004). High latitude ecosystems also play a significant role in the global carbon budget: large amounts of carbon are stored in widespread, often frozen, organic soils (Christensen et al. 1999), there are significant methane emissions from tundra wetlands (Christensen et al. 1996), and hundreds of thousands of lakes and ponds are reservoirs of organic carbon in water and sediment (Kling et al. 1991; Frey and Smith 2005). Species distributions in the Arctic are highly dependent on temperature, so amplification of global temperature change in this region will likely produce disproportionate impacts of vegetation patterns and related ecosystem function. Thus any amplified warming has potentially major ecological and socio-economic implications for Arctic areas (for example, IPCC 2001a, Chapter 16; Kaplan et al. 2003; ACIA 2004; Callaghan et al. 2004).

In turn, changing patterns of Arctic vegetation will almost certainly affect future climate through biophysical and biogeochemical feedbacks to the atmosphere-ocean system. Increases in tree and shrub cover would reduce total and seasonal albedo, warmer temperatures may increase carbon sequestration, and changes in the hydrological cycle due to melting permafrost could effect large changes in wetland area and methane emissions (Oechel et al. 1993; Foley et al. 1994; Bonan et al. 1995; Chapin et al. 1995; Christensen 1999; Chapin

[1] Greatest warming in GCMs is generally over the Arctic Ocean, while the largest warming in the observed record is over Northern Eurasia.

et al. 2000; Callaghan et al. 2005). Animals, and humans, would almost certainly also be affected by these vegetation changes (ACIA 2004).

The aim of this paper is to document the extent of climate and vegetation change in the Arctic under a global warming stabilization of 2 °C. This is a novel approach for examining future climate and environmental change: previous studies have focused on modeling future conditions under time-dependent increased greenhouse gas concentrations or doubled CO_2 scenarios, rather than assessing the regional implications of a specific global temperature stabilization target. Standardizing GCM data by a given global temperature target also removes some of the spread between GCM simulations relating to different emission scenarios and GCM sensitivities to forcing.

The paper begins with a description of our data sources, models and analysis methods. This is followed by sections that address the question of when a global 2 °C temperature change might occur, and what changes in climate (specifically temperature and precipitation) might be expected in the Arctic. We then describe the equilibrium response of Arctic vegetation to a global 2 °C temperature stabilization, as simulated using a state-of-the-art global biogeography-biogeochemistry model. Changes in sea-ice are not assessed, as these are addressed in detail in a recent report (Comiso 2005).

2 Data and methods

The methods used in this study had two major components, which we describe in turn: 1. identification of timing and patterns of Arctic climate change using an ensemble of GCM scenario simulations, and 2. simulation of Arctic vegetation cover under a 2 °C global warming using a vegetation model.

2.1 GCM data

Monthly data from six coupled ocean-atmosphere GCMs, each driven by several forcing scenarios, were downloaded from the IPCC Data Distribution Centre[2] (see Table 1). These models exhibit a range of sensitivity to greenhouse gas forcing, with transient climate responses (TCRs) ranging from 1.4 °C to 3.1 °C (Table 1). TCR is a measure of the GCM's sensitivity to CO_2 forcing (and by inference, total GHG forcing) and is defined by the IPCC (2001b, Figure 9.1) as the temperature change at the year of CO_2 doubling, when the climate model is forced by a 1% annual compound increase in CO_2 from preindustrial concentrations (as in the CMIP experiments). The models represent a subset of the range of models reported by the IPCC (2001b), but span nearly the full range of TCR of the larger IPCC group of models. Scenarios used to force these models were:

- The IS92a greenhouse gas only (IS92aGG);
- IS92a greenhouse gas plus aerosols (IS92aGS);
- SRES A2; and
- SRES B2.

This combination of models and scenarios permits a range of emissions scenarios and model responses to be assessed. In particular, it enables an evaluation of the sensitivity of Artic climate change to relatively high and low emission scenarios (and hence relatively

[2] http://IPCC-ddc.cru.uea.ac.uk.

Table 1 GCM-scenario combinations used in this study, and the Transient Climate Response (TCR) of each model

Model	TCR (°C)	Scenarios IS92aGG	IS92aGS	SRES A2	SRES B2
HadCM3[a]	2.0	√	√	√	√
ECHAM4[b]	1.4	√	√	√	√
CCSRNIES[c]	1.8/3.1 g	√	√	√	√
CGCM1[d]	1.96	√	√	–	–
CGCM2[d]	No data	–	–	√	√
GFDLR30[e]	1.96	–	–	√	√
CSIROMk2[f]	2.0	√	√	√	√

fast and slow rates of global climate change). Estimates of future CO_2 concentrations and total radiative forcing arising from these emissions scenarios can be found in IPCC (2001b, Appendix II). The scenarios used span nearly the full range of radiative forcing in the SRES marker scenarios at the time of global mean temperature change of 2 °C (2030s–2050s). Although other SRES scenarios were available for some models, the above are available across nearly all models, enabling a consistent analysis.[3] Control run[4] simulations were also available for each model; these are necessary to calculate the warming in each model relative to the model's preindustrial climate.

2.2 Time of 2 °C global temperature change

For each model, control-run surface temperature data were used to calculate a "pre-industrial" mean temperature climatology, and these were spatially averaged to calculate a global mean pre-industrial surface temperature. For each climate change simulation, the global temperature fields were spatially and temporally averaged to calculate time-series of global mean annual temperature, which were then differenced from the "pre-industrial" global mean temperature. The resulting global mean temperature-anomaly series were smoothed with a 21-year moving average, and the date at which the 21-year mean global temperature anomaly exceeded 2 °C was taken as the time of 2 °C global temperature change. The ECHAM4 IS92aGS simulation only ran to 2049, and did not reach a 2 °C global temperature change by the end of the simulation; consequently this run was excluded from much of the further analysis.

2.3 Arctic climate change at time of 2 °C global temperature change

All Arctic temperature and precipitation changes were expressed relative to the preindustrial mean climate for the model run in question. For each model, the thirty-one year mean monthly climate[5] centered on the time of 2 °C global temperature change was calculated

[3] Note that only SRES scenarios were available for the GFDLR30 model, while different versions of the CGCM and CCSRNIES models were used for the IS92 and SRES scenarios.

[4] A control run is a long (many hundreds of years) simulation where the CO_2 levels are specified at pre-industrial levels. Data from a control run are then used to determine the GCM's unforced climate, which serves as a reference against which simulations with enhanced levels of GHGs and aerosols can be assessed.

[5] A thirty-year mean is the "standard" time period used in many climate change studies, by the World Meteorological Organisation, and by the IPCC Data Distribution Centre. For the Arctic, where there can be natural variability on 10–20 year time scales, any thirty-year mean calculated at the time of a 2 °C global warming

and differenced from the control-run mean field. In the first instance, only near-surface temperature and total precipitation changes were analyzed.

The resultant change fields were summarized for all model simulations, using the common 0.5° latitude/longitude grid, by calculating the mean and standard deviation of all models on a grid-point by grid-point basis; these statistics were calculated for monthly, seasonal and annual fields.

Changes in area-mean temperature and precipitation in the Arctic (here defined as latitudes >60°N) were calculated from these fields using area-weighted averaging. Rates of change at the time of 2 °C warming were also estimated, by calculating the linear trend in temperature for the 41-year period centered on the year of 2 °C global warming. These rates were determined for both area-mean temperature and at individual GCM grid points.

2.4 The arctic region and arctic grid

For the vegetation modeling experiments, the area defined as the Arctic was established by combining the Arctic boundary polygons of the Arctic Monitoring and Assessment Program (AMAP[6]) and Conservation of Arctic Flora and Fauna (CAFF[7]), using the southernmost defined boundary at any given point (Figure 1). This polygon defines the Arctic to cover northernmost Fennoscandia, northern European Russia, Siberia north of approximately 65°N, all of the Chutkotka peninsula, and most of Alaska. In Canada, the boundary of the Arctic includes all of Yukon Territory and the Mackenzie river valley, a zone of several hundred km surrounding Hudson Bay, and Quebec south to ca. 52°N. All of Greenland, Iceland, and Svalbard, as well as the smaller North Atlantic and Arctic islands are also covered by this definition.

The Arctic polygon was projected to a north polar aspect Lambert Equal-Area projection and gridded at 10 km resolution. As described below, climate and land surface properties, a map of observed natural vegetation, and vegetation model output were projected and interpolated to this grid. The Arctic grid has nearly 1 million grid cells, of which ca. 13.1×10^6 km^2 is ice-free land area. For analysis of regional changes in vegetation, we divided the total Arctic area into zones (Figure 1) roughly relating to areas with climatologic, topographic, or pedologic similarity (Kaplan et al. 2003).

2.5 Arctic vegetation classification and observed distribution

As a baseline to study the effect of warming on the vegetation of the Arctic, we created a unified vegetation classification and assembled a map of present-day observed vegetation using this classification. This map of observed Arctic vegetation is used to evaluate a model simulation for the present-day. The model is then used in turn to investigate potential Arctic vegetation change under global 2 °C warming scenarios.

To create a unified Arctic vegetation classification, we combined a standardized circumarctic scheme for tundra at the biome level (CAVM-Team 2003; Kaplan et al. 2003; Walker et al. 2005) with existing global vegetation classifications used by modelers (Kaplan 2001) and remote sensing based land cover datasets (JRC 2003). Each biome is defined

will likely contain a proportion of decadal-scale natural variability, as one might expect in the real world in the next century.

[6] http://www.amap.no.

[7] http://www.caff.is.

Fig. 1 Arctic boundary and zones used in the vegetation modeling experiments

in terms of physical structure and dominant life forms, is floristically distinguishable and occupies a unique and definable climate space. The global scheme used here distinguishes five tundra biomes along with cool and cold forest biomes (Kaplan 2001), and a mixed shrub tundra-forest biome (cold parkland). The tundra biomes are: low- and high-shrub; erect dwarf-shrub; prostrate dwarf-shrub; cushion forbs, lichen and moss; and graminoid and forb.

Using this classification, we prepared a vegetation map of observed present-day Arctic vegetation by combining information from remote sensing based data sources. Tundra vegetation distribution is based on the Circumpolar Arctic Vegetation Map (CAVM-Team 2003; Walker et al. 2005). The distribution of other vegetation types and the location of the forest limit were defined from the Global Land Cover 2000 (GLC2000) map (JRC 2003), with minor modifications of nomenclature. The CAVM and GLC2000 maps have been created primarily from original remote sensing data, and were interpreted and classified by regional experts. Both source maps have been subject to extensive ground truthing and accuracy analysis. The

resulting composite map may be considered the best currently available. Importantly, this map does not contain any assumed bioclimatic relationships or model and so provides an independent verification of model results for the present day.

2.6 The BIOME4 model

BIOME4 is a coupled carbon and water flux model that predicts steady state vegetation distribution, structure, and biogeochemistry, taking into account interaction between these effects (Kaplan 2001). The model is the latest generation of the BIOME series of global vegetation models, which have been applied to a wide range of problems in biogeography, biogeochemistry, and climate dynamics (Prentice et al. 1992; VEMAP 1995; Christensen et al. 1996; de Noblet et al. 1996; Haxeltine and Prentice 1996a; 1996b; Jolly and Haxeltine 1997; Harrison et al. 1998; Kaplan 2002; Kaplan et al. 2002). BIOME4 has been specifically developed with the intent improved simulation of cold-climate, high latitude vegetation (Kaplan et al. 2003). While BIOME4 can be run for any area and at any spatial resolution, the model is generally designed to be used at continental to global scales.

Twelve plant functional types (PFTs) in BIOME4 represent broad, physiologically distinct classes, ranging from cushion forbs to tropical broadleaf trees (Kaplan 2001). Each PFT is assigned a small number of bioclimatic limits which determine whether it could be present in a given grid cell, and therefore whether its potential net primary productivity (NPP) and leaf area index (LAI) are calculated. The PFTs also have a set of parameter values that define its carbon and water exchange characteristics. The computational core of BIOME4 is a coupled carbon and water flux scheme that determines the seasonal maximum LAI that maximizes NPP for any given PFT, based on a daily time step simulation of soil water balance and monthly mean calculations of canopy conductance, photosynthesis, respiration and phenological state (Haxeltine et al. 1996). The model is sensitive to CO_2 concentration because of the responses of NPP and stomatal conductance to CO_2.

To identify the biome for a given grid cell, the model ranks the tree and non-tree PFTs that were calculated for that grid cell. The ranking is defined according to a set of rules based on the computed biogeochemical variables, which include NPP, LAI, mean annual soil moisture, and an index of vulnerability to fire. The resulting ranked combinations of PFTs lead to an assignment to one of 27 global biomes of which the tundra and cold forest biomes described above are a subset (Figure 8). The 28th cover type, ice sheets and glaciers, is prescribed.

2.7 Vegetation model input data

BIOME4 uses climatological mean fields of monthly temperature, precipitation, and surface irradiance or cloudiness. In addition, the model requires information on the ambient mean atmospheric CO_2 concentration, and soil texture in the surface and subsoil, and soil depth. Preparation of baseline and scenario datasets for the vegetation model simulations are described below.

2.7.1 Baseline climatology

We used a gridded long-term mean climatology of temperature, precipitation, and surface shortwave insolation for the late 20th century for the present-day vegetation simulation and as a baseline for the two-degree warming experiments. Temperature and precipitation data

are from the CRU CL 2.0 dataset, which is a mean over the period 1961–1990 (New et al. 2002). The CRU CL 2.0 dataset is on a 10' geographic grid, which represents a horizontal grid-node spacing of approximately 10 km at 60°N. Because of very sparse station density, particularly in the Arctic, in the CRU CL 2.0 interpolated fields of cloudiness, and suspected inaccuracies in using these data with BIOME4 (Kaplan et al. 2003), we have used a dataset of surface shortwave insolation from the ISCCP/SRB project[8] instead (1983-1995 mean). This dataset combines satellite-based observations of clouds with a sophisticated atmospheric radiative transfer scheme to produce surface insolation fields and is an improvement over previous, parameterized approaches (Kaplan et al. 2003). Although the ISCCP/SRB data covers a different time period than the temperature and precipitation fields and is on a somewhat coarse, 280 km equal-area grid, the paucity of climate stations and unreliability of using cloudiness data for approximating surface insolation in high latitudes makes use of this dataset an improvement of previous sources. Additionally, as cloudiness is not a regular output of GCMs, but surface insolation is, the use of a surface insolation baseline dataset simplified the calculation of future climate fields. Both datasets were projected to the 10 km Arctic grid using bilinear interpolation.

2.7.2 Two-degree warming scenarios

Four future climate scenarios which represent different realizations of Arctic climate under a 2 °C global warming were prepared for the vegetation model experiments. The scenarios are derived from the ensemble of seven GCMs forced by the series of different emissions scenarios described in previous sections.

The four scenarios represent 80% of the range in the amplitude of local temperature and precipitation anomalies in the Arctic: 10th percentile, 90th percentile, simple mean and robust mean. The method for calculating the percentiles assumed that the ensemble data at each grid point were normally distributed. To the ensemble mean, z standard deviations were added or subtracted, where z corresponds to a cumulative probability of 0.10 for the standard normal distribution. To calculate a robust estimate of the ensemble mean changes, a "robust mean" scenario was defined. This robust mean is a weighted average of each of the 10th, 25th, 50th, 75th and 90th percentiles,

$$R = 0.0833 * p10 + 0.2083 * p25 + 0.4166 * p50 + 0.2083 * p75 + 0.0833 * p90$$

where R is the robust mean value and $p10$, $p25$, etc. are the percentile values as calculated above. The four scenarios thus cover 80% of the range in the magnitude of the Arctic temperature and precipitation anomalies under a 2 °C global warming, with the 10th percentile having smallest temperature change from control, i.e. "coolest," followed in magnitude of the temperature anomaly by the robust mean, simple mean, and 90th percentile or "warmest." The climate anomalies were projected onto the 10 km Arctic grid using bilinear interpolation.

2.7.3 Earth surface properties and CO_2 concentration

Land areas and glacier coverage in BIOME4 were defined by combining the FAO digital soil map of the world (FAO 1995) with the Circum-Arctic Vegetation Map (CAVM-Team 2003; Walker et al. 2005). The land ice area defined by the CAVM was considered definitive. The soil

[8] http://eosweb.larc.nasa.gov/PRODOCS/srb/table_srb.html.

properties used by BIOME4 (water holding capacity and saturated hydraulic conductivity) were taken from the maps of derived soil properties based on the FAO soil map and pedon databases (Reynolds et al. 1999). For areas not covered by the FAO and derived properties maps, including Svalbard and Russian Arctic islands, characteristic soil physical properties were estimated (e.g. for cryosols).

In the experiments with BIOME4, we did not attempt to estimate changes in land surface properties. This particularly applies to ice coverage, where retreat or melting of Arctic land ice was not considered. Pedogenesis and soil erosion were not considered in this model analysis either. While these geomorphic processes are important on century to millennial time scales, it was beyond the scope of the current research to attempt to model them because of lack of driving data and technical complexity.

The ambient mean-annual CO_2 concentration used by the model in the present-day scenario reflects a mid-20th century mean of 324 ppm. In future scenarios, we used a CO_2 concentration of 475 ppm, which is approximately the atmospheric CO_2 concentration calculated by a simple coupled carbon cycle model (Joos et al. 2001) in the mean year of the 2 °C warming (i.e. year 2043). Though some of the extreme climate scenarios were produced by higher CO_2, previous work has shown that Arctic vegetation is much more sensitive to climate changes than to the direct effect of increased CO_2 concentrations above 20th century levels (Kaplan et al. 2003).

3 Results

3.1 Time of 2 °C global temperature change

The time at which the simulated global mean temperature exceeds the control run global mean by 2 °C ranges from between 2026 and 2060 (Figure 2). The inter-model spread for a single scenario (e.g. B2) is nearly as large as the total spread; however, there is a tendency for the simulations forced by scenarios with greater accumulated radiative forcing (IS92aGG, A2) to exhibit a greater rate of warming, and reach the 2 °C threshold earlier.

3.2 Arctic-wide climate change at the time of 2 °C global warming

The co-evolution of global and Arctic (defined as latitudes greater than 60°N) area-mean temperature is shown in Figure 3. Most models show a similar response, with Arctic temperature change ranging between 3.2 °C and 4.5 °C at the time of a 2 °C global warming; however, the CCSRNIES model shows a stronger response, with a change of up to 6.6 °C. In all models, Arctic temperature change through time is approximately a linear function of global temperature change. This would suggest that, for the amounts of global warming simulated by these models over the next 100 years, the nature of the feedbacks causing Arctic amplification in a specific model remain the same. As noted previously, the dominant feedback causing the temperature amplification in the CMIP simulations of these models is related to sea-ice. If warming proceeds until a model has little remaining sea ice, the ice-albedo feedback would necessarily reduce, and the linearity reported here may break down.

The similar relationships between global and Arctic temperature change across most of the GCMs suggest that the relative size of Arctic temperature amplification does not depend strongly on the rate of global warming, at least for rates of warming arising from the forcing scenarios evaluated here. Some models show greater amplification when forced by lower-emissions scenarios while others show more amplification under higher emission

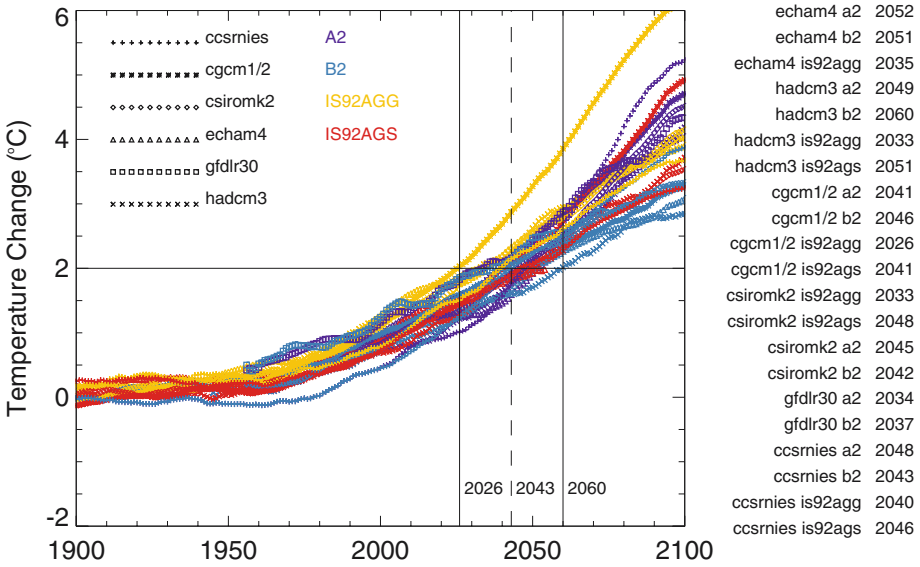

Fig. 2 Global mean annual temperature anomalies relative to "preindustrial" control climatology, smoothed with a 21-year moving average. Vertical lines indicate the range (solid) and median (dashed) time at which the 21-year global mean temperature anomaly exceeds +2 °C. Figures on the right show the time at which the 21-year mean global temperature anomaly exceeds +2 °C for each GCM-scenario combination

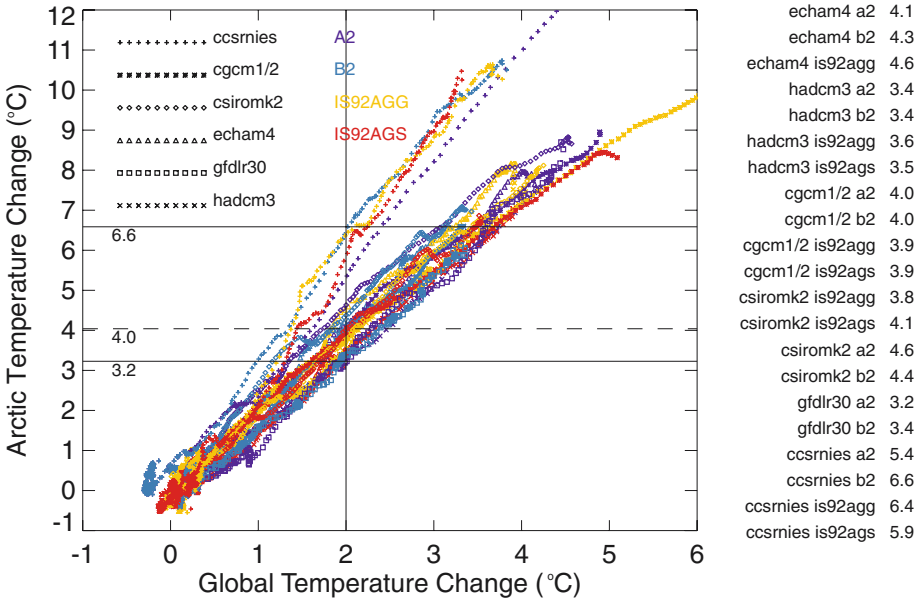

Fig. 3 Co-evolution of global and Arctic annual temperature anomalies from "preidustrial" CO_2 concentrations through to 2100, smoothed with a 21-year (31-year for the Arctic) moving average. Horizontal lines show the range (solid) of and median (dashed) temperature changes predicted for the Arctic when the global temperature anomaly reaches 2 °C. Figures to right list the 31-year mean annual Arctic temperature change at the time of 2 °C global warming for each model

Table 2 The mean Arctic temperature amplification, and the rate of temperature change, at the time of a global mean warming of 2 °C for each model-scenario combination. The rate of change is calculated over a 41-year period centered on the time of 2 °C global warming

Model	Scenario	Arctic amplification (°C/°C)	Arctic rate of change (°C/decade)
ECHAM4	A2	1.9	0.74
ECHAM4	B2	2.0	0.52
ECHAM4	Is92agg	2.1	0.58
HadCM3	A2A	1.8	0.69
HadCM3	B2A	1.9	0.48
HadCM3	Is92agg	1.9	0.59
HadCM3	Is92ags	2.0	0.62
CGCM2	A2	1.9	0.68
CGCM2	B2	1.9	0.42
CGCM1	Is92agg	1.7	0.72
CGCM1	Is92ags	1.7	0.63
CSIROMK2	Is92agg	2.1	0.60
CSIROMK2	is92ags	2.1	0.58
CSIROMK2	A2	2.0	0.73
CSIROMK2	B2	1.9	0.50
GFDLR30	A2	2.0	0.60
GFDLR30	B2	1.9	0.45
CCSRNIES	A2	2.8	1.55
CCSRNIES	B2	3.0	1.09
CCSRNIES	IS92agg	3.0	0.95
CCSRNIES	IS92ags	3.4	0.92

scenarios. Differences in the amplification are, if anything, more dependent on differences between the models themselves (Table 2). For any model, scenarios with faster (slower) global warming also show faster (slower) Arctic warming, but the Arctic amplification is similar for fast and slow warming scenarios. Thus, in each model, the temperature change in the Arctic when the global temperature change reaches 2 °C will be similar regardless of when this global change occurs. There may be additional lags in the Arctic climate system (e.g. changes to permafrost and vegetation cover) that will only become apparent later, but over the timescales considered here, the snow/ice albedo feedback shows the strongest relationship to temperature change (Holland and Bitz 2003; Flato 2004), and is likely to be dominant.

Far more significant, is the rate of temperature change in the Arctic at the time of 2 °C global warming (Table 2). For the models with broadly similar Arctic temperature amplification (i.e. all models except CCSRNIES), differing climate sensitivities and forcing produce rates of change in area-average Artic temperature that range from 0.45 to 0.75 °C/decade. Although the CCSRNIES model has the largest amplification of Arctic temperature change, and therefore produces the fastest rates of Arctic temperature change, these are large – between 0.92 and 1.55 °C/decade. The highest rate of 1.55 °C/decade is interesting, as it is partly due to a regional warming in the Arctic that is much faster than the longer-term rate (Figure 3). Although the cause of this period of above average warming is unclear (it could be an abrupt change caused by overall warming or, more likely, natural variability superimposed on the underlying global-warming signal), it does suggest that over decadal time scales, there can be extreme rates of regional warming. Periods of more rapid Arctic

temperature change are evident from a number of different model runs at various times (Figure 3).

Changes in seasonal mean temperature are largest in winter and autumn and lowest in summer (Figure 4). The median change in temperature in the winter is 6.2 °C, approximately 1.5 times the annual change in the Arctic and three times the global mean change. The reduced warming in summer is fairly well understood (IPCC 1995); where sea-ice remains, most additional atmospheric heat is consumed by surface melting, and where sea-ice is removed, the thermal inertia of the ocean mixed layer suppresses near-surface air

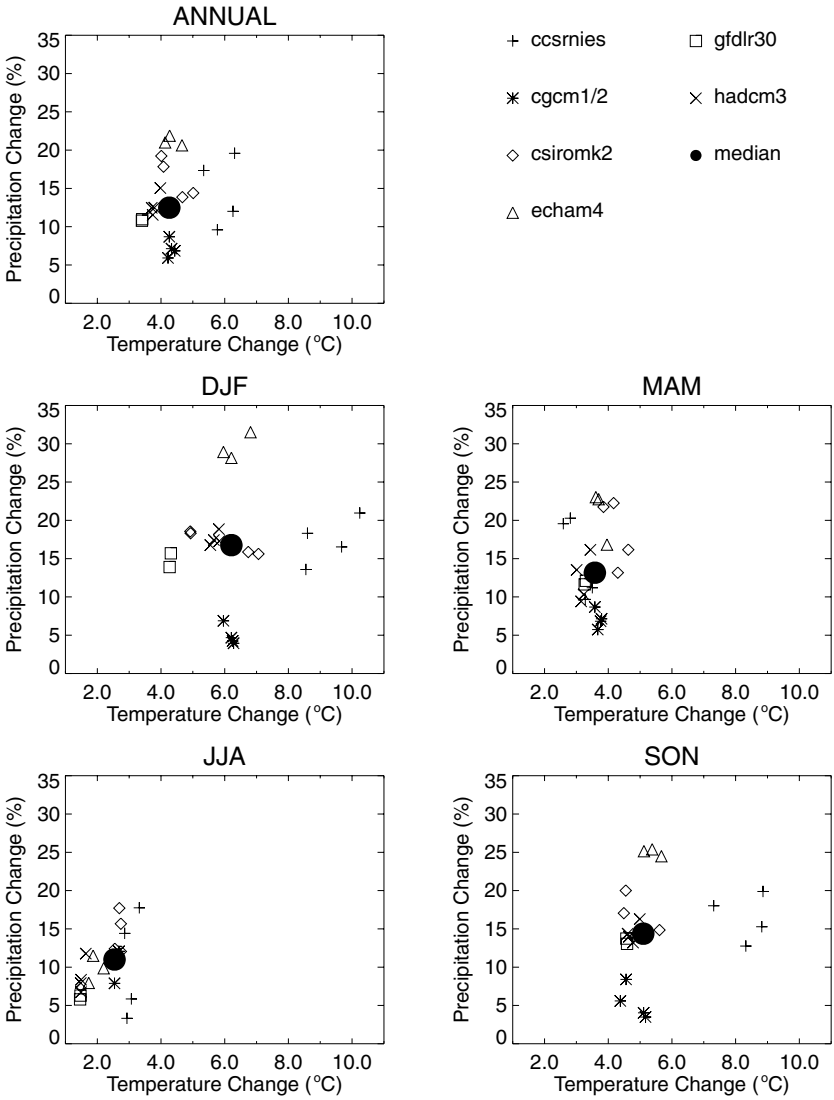

Fig. 4 Seasonal changes in area-weighted mean temperature and precipitation over the Arctic at the time of a global 2 °C warming

temperature increases. The marked seasonality in the amount and rate of change has important implications for the impacts of climate change in the Arctic. Natural processes and human activities that are dependent on winter temperature are likely to be more severely affected.

Area-average precipitation change is always positive, but varies considerably from model to model. Annual precipitation change varies from +5% to +22%, with a median change of +12%. Changes in precipitation in each season have roughly similar ranges, with maximum changes of just over +30% in DJF and +18% in JJA (Figure 4). There is a slight hint of a correlation between rainfall and temperature change, as noted at the global scale by Allen and Ingram (2002) and for the Arctic by Raisanen (2001b), but the relationship for the models studied here is weak and not statistically significant. Raisanen's analysis of 19 CMIP2 models showed a much stronger relationship between temperature and precipitation change in the Arctic. This is partly because his study included more models, some of which had a greater range of predicted temperature and precipitation changes, strengthening the weak relationship seen with the models used here, but also because this study includes results from four simulations with each model. Inspection of Figure 4 shows that between-model variations in precipitation change can be quite large (e.g., from 10% to 20% for HadCM3), which adds considerable noise to the temperature-precipitation relationship.

3.3 Regional patterns of climate change

3.3.1 Temperature

The median pattern of temperature change in the Arctic at the time of 2 °C global warming simulated by each GCM is illustrated in Figure 5, and summarized for all GCMs in Figure 6. These figures illustrate areas of agreement and disagreement between model results. While there are significant inter-model differences, both in the amount of warming and its distribution, there are a number of similarities worthy of mention. The largest warming in annual temperature is generally located in the central Arctic Ocean. This warming is primarily due to large positive anomalies in winter. In summer, the Arctic Ocean generally warms less than the surrounding land areas. The other common pattern is a lower warming or even a cooling in the North Atlantic. This pattern is most pronounced in HadCM3, but is present in all models, and is often related to the weakening of the Atlantic thermohaline circulation. Local anomalous areas of cooling or large warming in individual models are most likely related to changes in the sea-ice characteristics relative to the control simulation. There is no relationship between the Arctic-wide average rate of warming and the spatial patterns of warming; patterns appear to be dominated by model-specific responses.

Rates of change also show significant spatial variability. Areas with larger temperature anomalies tend to be associated with greater rates of change (as expected). Annual average temperature changes at rates of approximately 1 °C and 0.5 °C per decade over the Arctic Ocean and surrounding continental areas respectively. In winter, where the sea-ice feedback produces large changes in temperature over the Arctic Ocean, average rates of temperature change are similarly elevated, ranging from about 1.5 °C per decade at the ocean margins to 2.7 °C per decade in the interior of the ocean. In summer, rates of warming are lowest over the Arctic Ocean and range between 0.25 and 0.5 °C per decade of polar land areas. The

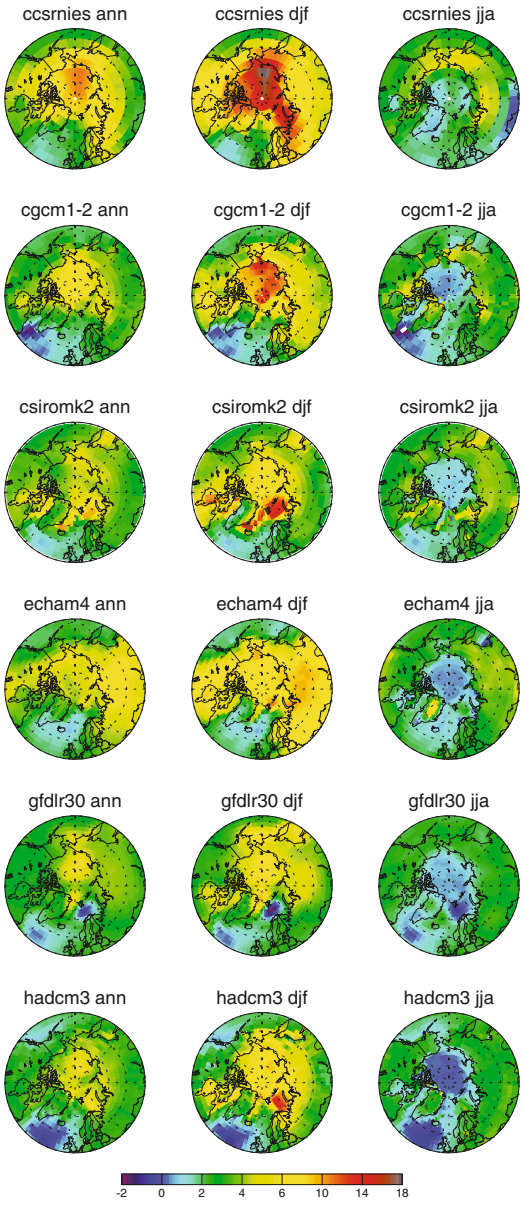

Fig. 5 Median annual, winter and summer temperature changes (°C), relative to control (pre-industrial) climatology, at the time of a global warming of 2 °C, calculated from the range of changes simulated by each GCM forced by the four (three for ECHAM4 & two for GFDLR30) emissions scenarios. Note that the map domain extends from 50°N

range in warming rates varies considerably in areas with the largest rates of change, so these median estimates of the average rate of change have large confidence bounds.

3.3.2 Precipitation

The broad patterns of precipitation change are similar between models (Figure 7), although the absolute amounts of change are quite varied, and depend to some extent on the amount of rainfall in the control simulations ("wetter" models tend to have larger absolute changes

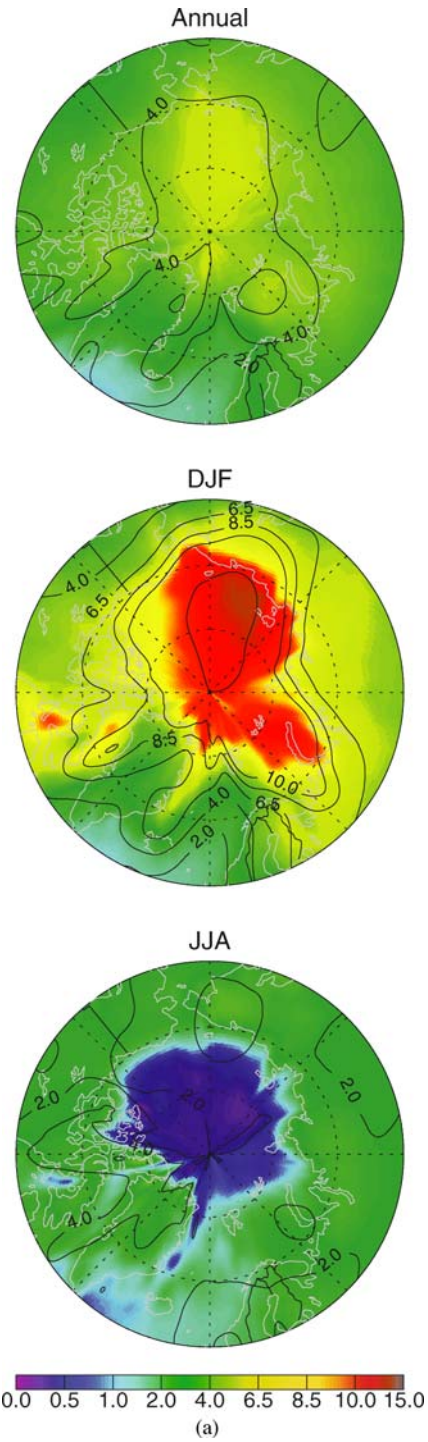

Fig. 6 Summary of annual and seasonal temperature changes and rates of change over the Arctic at the time of 2 °C global warming, as simulated by the GCMs used in this study. (a) Median (colors) and range (lines) of mean temperature change, in °C. (b) Median (colors) and range (lines) of the rate of temperature change, in °C per decade. Note that some of the linear features on the map arise from interpolation of GCM data with different spatial resolution to a common grid (*continued on next page*)

Fig. 6 (*Continued*)

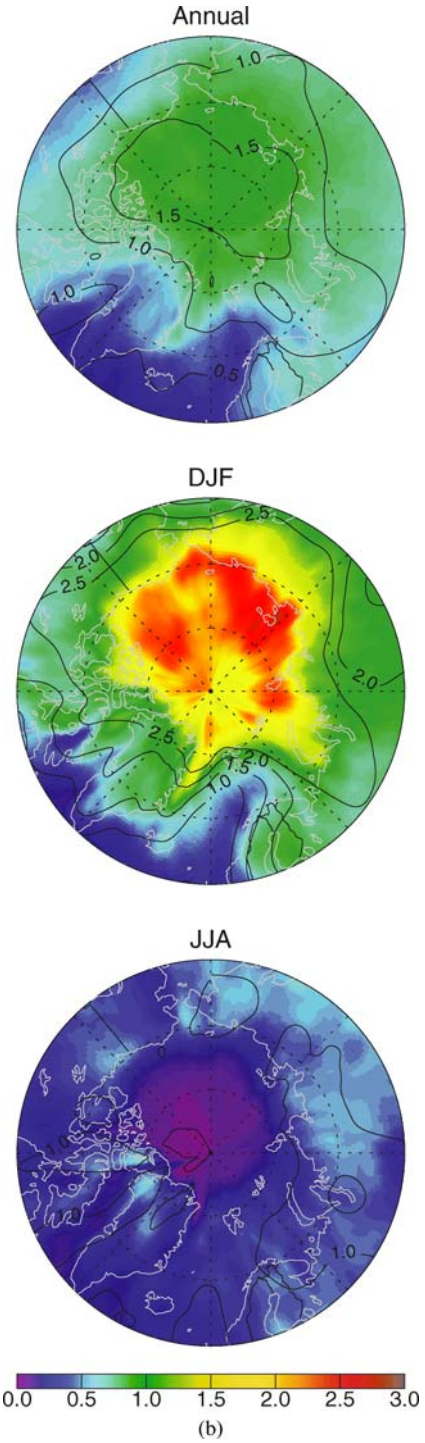

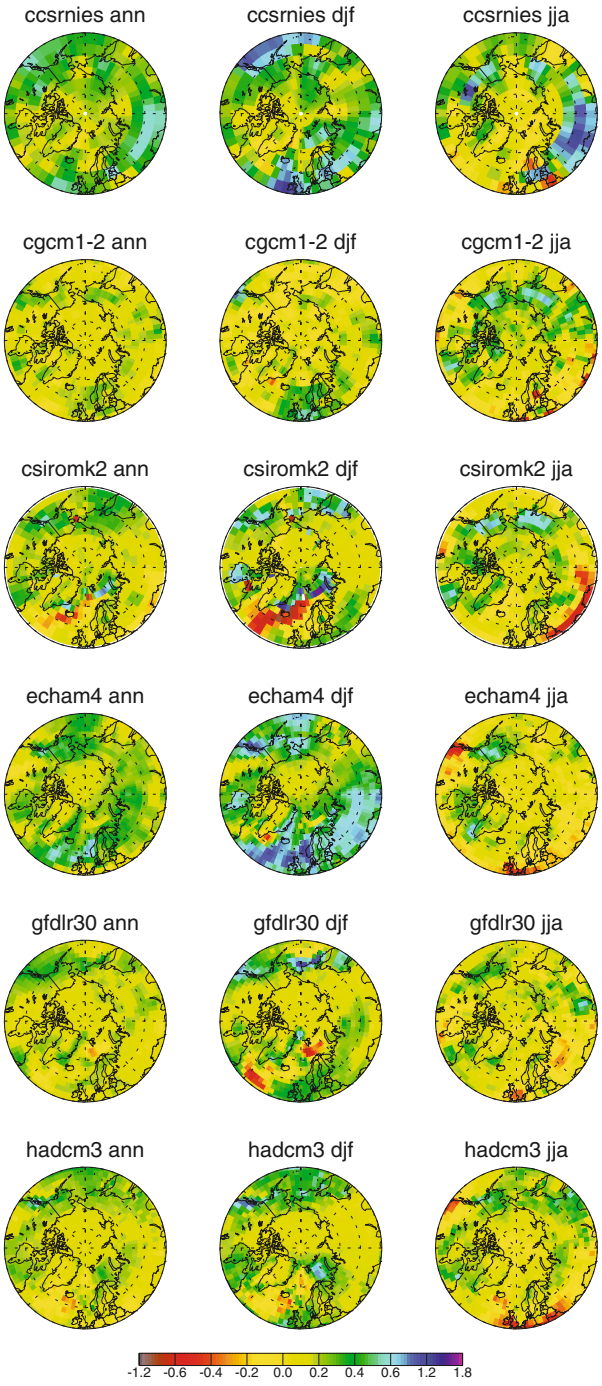

Fig. 7 Median annual, winter and summer precipitation changes (in mm), relative to control (pre-industrial) climatology, at the time of a global warming of 2 °C, calculated from the range of changes simulated by each GCM forced by the four (three for ECHAM4 & two for GFDLR30) emissions scenarios. Note that the map domain extends from 50°N

in precipitation). All models simulate a general increased precipitation over most of the Arctic; HadCM3, GFDLR30 and CSIROMk2 show reduced rainfall over the North Atlantic and/or Greenland seas that correlate with areas with the smallest or negative temperature changes. There is some tendency for largest absolute precipitation changes to be over the land areas, but the loci of these maxima vary between models to the extent that there is very little commonality. The greater changes over land is at least in part due to the due to the fact that GCM precipitation is larger over sub-Arctic continents (at ∼50–70°N) than over the Arctic Ocean. Model simulations generally show the largest relative (percent) increase in precipitation over the Arctic Ocean (c.f., Raisanen 2001a).

Reasons for overall increased precipitation over the Arctic are thought to relate primarily to enhanced advection of moisture from lower latitudes by a warmer troposphere, as evaporation (and hence a local moisture source) is very low in the Arctic. Indeed, the largest relative changes occur over the central Arctic Ocean (Raisanen 2001b) in winter and autumn, where evaporation is effectively zero, and any increase in moisture will have the largest relative effect. The spatial patterns of precipitation change are likely due to a combination of overall increased moisture advection in to the region and changes in circulation that are to some extent model-specific. For example, Rauth and Paeth (2004) have shown that changes in the dominant modes of Northern Hemisphere atmospheric variability (Arctic Oscillation, NAO and Aleutian Low) contribute a significant proportion of local changes in precipitation in the Arctic.

3.4 Vegetation cover and change

3.4.1 Present day natural vegetation

The vegetation of the Arctic is characterized by a transition from boreal forests to tundra shrublands that become progressively shorter in stature farther north. The coldest and most northerly parts of the Arctic are sparsely vegetated by cushion forbs, lichens and moss, and dominated by rocky barrens or permanent ice fields and glaciers.

In a quantitative comparison between the modern observed vegetation map (Figure 8a) and present-day vegetation distribution simulated by BIOME4 (Figure 8b), 65.0% of grid cells (84036 grid cells excluding ice covered areas) matched in biome classification. Percentage matching for grid cells assigned to specific forest biomes in the observed vegetation map were: cold evergreen needleleaf forest, 76.9%; cold deciduous forest, 77.7%; cold parkland, 91.0%. The biome cold parkland is a transition biome between cold evergreen forest and high and low shrub tundra. While not specifically classified in the observed vegetation map, where cold parkland was simulated by BIOME4 it was considered a match to the observed map when either cold evergreen needleleaf forest or high and low shrub tundra was simulated. In those regions where the model incorrectly simulates forest, primarily in hypermaritime south-western Alaska and in Chukotka, the influence of cool summer temperatures, permafrost, and waterlogged soils may suppress the growth of trees in a way that is not accounted for by the model. Future versions of the BIOME model will include simulation of wetlands and permafrost and may alleviate this discrepancy.

Among the tundra biomes, high- and low-shrub tundra matched the observed map at 60.3% of the 10 km grid cells, erect dwarf-shrub tundra 43.2%, prostrate dwarf-shrub tundra 40.9%, and cushion forb, lichen, and moss tundra 26.2%. Major differences between the observed vegetation map and the simulation relate to the widespread observation of barren areas in Keewatin and on Baffin Island that were simulated as tundra vegetation by the model. This discrepancy is a product of the soils data used by the model, where a soil profile was defined

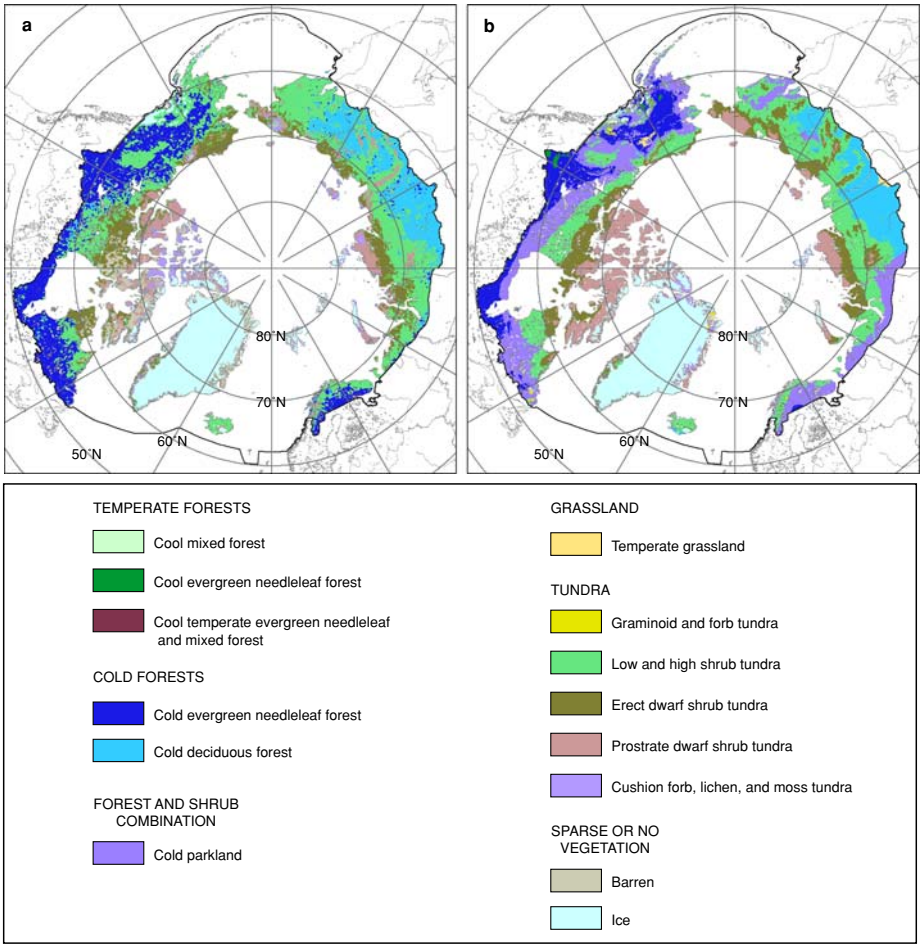

Fig. 8 Arctic vegetation of the present day, a observed in the combined CAVM/GLC2000 dataset, and b simulated by BIOME4 using late 20th century climatology. The legend is used for all vegetation maps

for these areas when in fact much of the area is barren because it is exposed bedrock. Work to improve circumpolar soils mapping is ongoing, and new soils maps may lead to better predictions of barren areas in Canada.

Other areas of disagreement include the under-simulation of the area of cushion forb lichen and moss tundra in the far northern Canadian archipelago, where prostrate dwarf-shrub tundra is simulated instead. The few temperature measuring stations in this region are located in sheltered or low-elevation areas and may be responsible for warmer than actual temperatures in the driver data set (New et al. 2002; Kaplan et al. 2003), which would favor the shrub tundra over cushion forbs, lichen and moss tundra, which is found in only the harshest environments. Finally, the model tended to underestimate the area of prostrate dwarf-shrub tundra and cushion forb lichen and moss tundra in mountain regions, particularly in eastern Siberia. The model predictions of forest where none is observed today could result in an overestimate of forest area in the 2 °C warming scenarios, as similar edaphic controls on forest distribution are likely to exist in other areas of the Arctic. Similarly, the under-prediction

of the area of cushion forb tundra at the present could lead to its extent being under-predicted in climate change scenario experiments.

3.4.2 Equilibrium vegetation changes under global 2 °C warming

In our four scenarios of a global 2 °C warming the potentially forested area of the Arctic increases significantly (Table 3). The increase in forest area ranged from ca. 13% to nearly 90%, with a mean value approaching an increase in area of 9×106 km^2. Forests reach the Arctic coastline in all but the 10th percentile "cold" scenario (Figure 9). Trees are shown potentially invading Greenland and Chukotka, where only fragments of forest exist today (Table 4). In the 90th percentile "warm" simulation the area of cold deciduous forest is strongly reduced by replacement with evergreen forests (Figure 10), a result also found in other studies (Cramer et al. 2001; Kaplan et al. 2003). In the three warmest scenarios, there is a large increase in temperate forest area in the Arctic, concurrent with expansion of the cold forest types; the overall expansion in forest area is largely at the expense of the tundra.

Table 3 Changes in Arctic biome area under 2 °C warming scenarios

	Forest		Tundra		Other	
	km^2 × 1000	% Change	km^2 × 1000	% Change	km^2 × 1000	% Change
Present	5591.6		7366.2		136.5	
10th percentile "cool"	6314.5	12.9	6659.2	−9.6	120.6	−11.6
Robust mean	8710.3	55.8	4275.0	−42.0	109.0	−20.1
Mean	8839.2	58.1	4148.1	−43.7	107.0	−21.6
90th percentile "warm"	10485.7	87.5	2455.9	−66.7	152.7	11.9

Table 4 Percent changes in Arctic biome area by region. Percentage change in forest area in Greenland is very high because the small area of forest simulated in the control simulation (200 km^2)

	10th percentile "cool"		Robust mean		Mean Mean		90th percentile "warm"	
	Forest	Tundra	Forest	Tundra	Forest	Tundra	Forest	Tundra
Alaska	5.1	−12.6	24.4	−64.9	24.7	−66.7	25.9	−86.7
Mackenzie	5.9	−19.9	15.1	−50.9	15.8	−53.3	24.8	−83.5
Keewatin	5.0	−1.6	38.2	−12.1	42.3	−13.4	103.6	−32.8
Labrador	7.0	−4.7	50.1	−37.9	52.7	−39.9	80.4	−61.5
Greenland	3000.0	−7.7	19050.0	−17.4	20050.0	−17.8	40200.0	−34.3
Atlantic	11.9	−7.2	236.5	−44.5	251.6	−44.8	511.9	−73.1
Western Europe	18.2	−42.2	37.2	−88.1	37.5	−88.9	38.8	−99.6
Eastern Europe	−21.0	27.7	50.7	−66.6	52.0	−68.4	62.8	−82.6
Western Siberia	36.9	−14.8	154.9	−62.3	158.9	−64.0	229.4	−92.3
Taymyr	37.4	−28.1	81.3	−61.1	82.1	−61.7	102.8	−77.3
Lena	25.7	−56.2	38.1	−100.0	38.1	−100.0	38.1	−100.0
Eastern Siberia	31.3	−10.9	149.0	−52.4	157.5	−55.6	240.6	−87.7
Chukotka	−29.9	8.6	123.3	−37.1	131.2	−39.5	239.7	−72.0

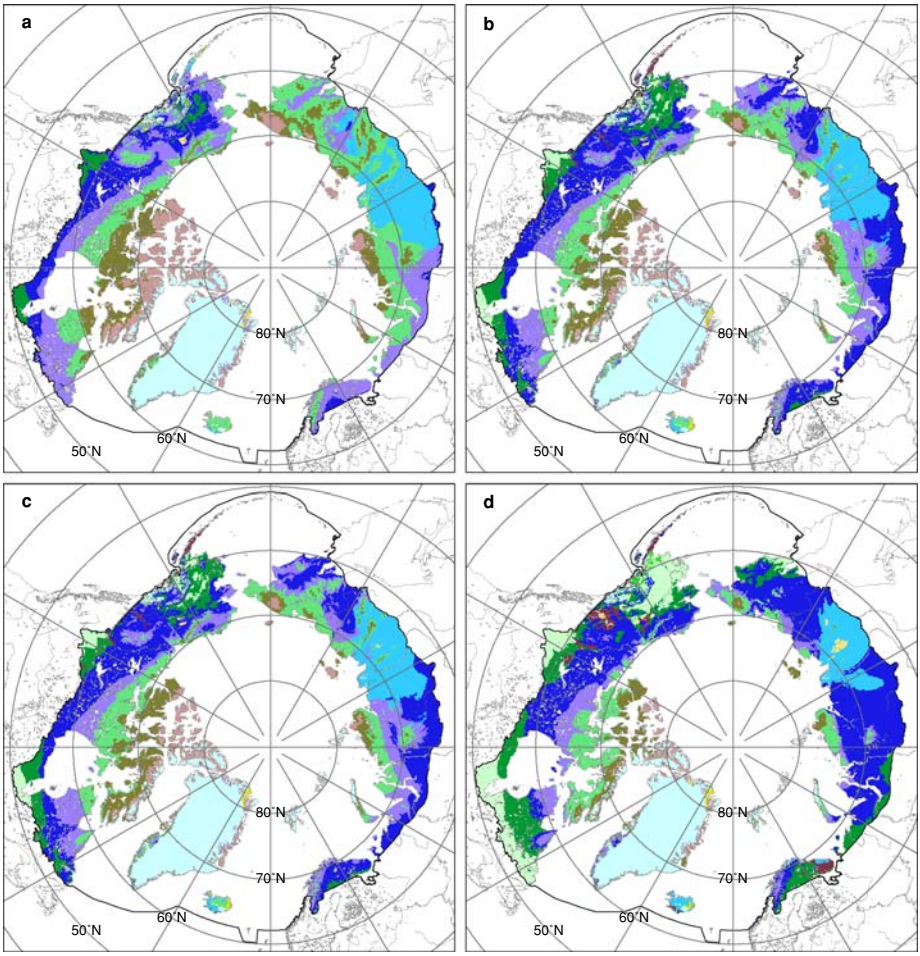

Fig. 9 Simulated Arctic biomes under a 2 °C global warming in a the 10th percentile "cool" scenario, b the robust mean scenario, c the simple mean scenario, and d the 90th percentile "warm" scenario

The 2 °C warming simulations show major northward shifts of the shrub-dominated tundra biomes, with major reductions in the total area of erect and prostrate dwarf-shrub tundras, in many cases below 1 × 106 km2 (Figure 11). Cushion forb, lichen and moss tundra is nearly extinct in all but the coldest scenario, though this type of tundra would presumably be the first to occupy areas are vacated by melting icecaps and glaciers, which were not considered in this study. The tundra biomes become restricted to coastal and mountainous areas of the Arctic, disappearing almost completely from regions such as Western Europe and the Lena River valley, and with significant reductions in Alaska, Eastern Siberia, and the Mackenzie drainage. The area of cold parkland is reduced in the three warmest scenarios, where it is mostly replaced by forest. In some areas with steep climatic gradients, such as along coastlines, the cold parkland is equally replaced by forest and tundra.

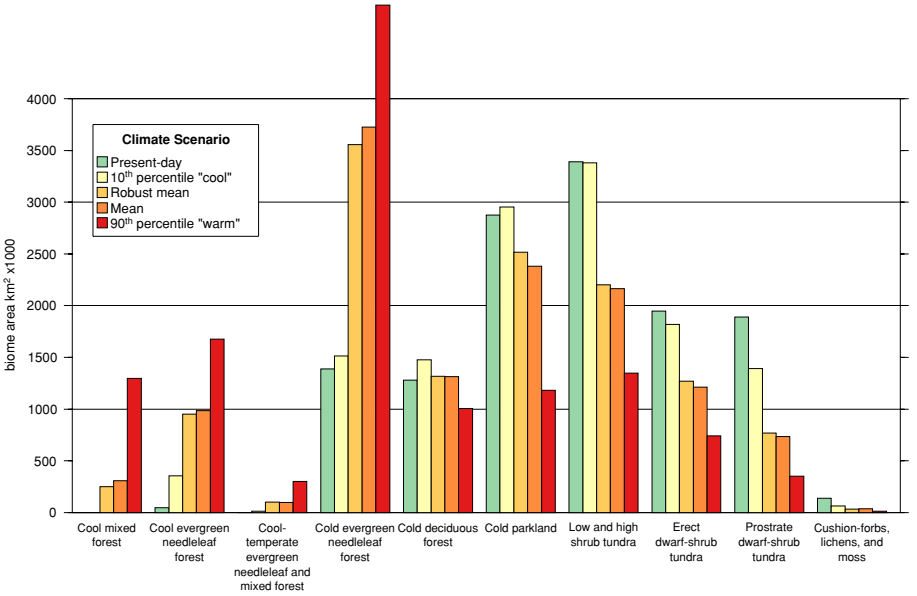

Fig. 10 BIOME4 simulated area of Arctic biomes at present and under 2 °C warming scenarios

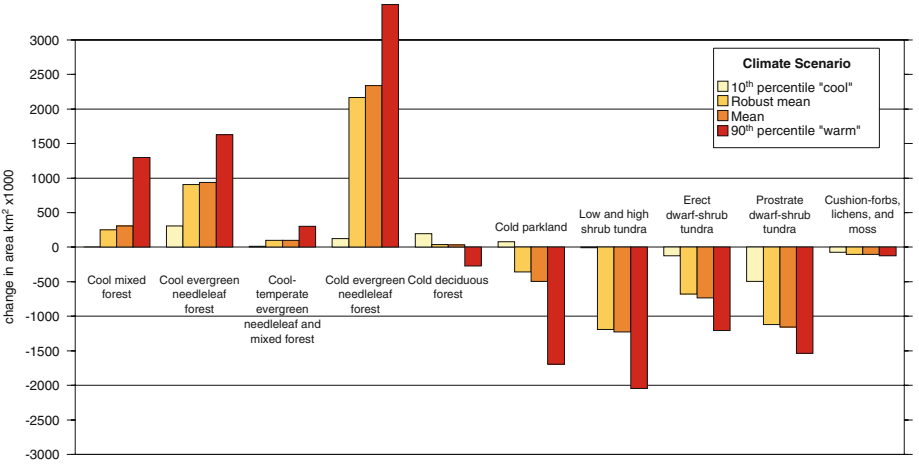

Fig. 11 BIOME4 simulated area change of biomes under 2°C warming scenarios

3.4.3 Biogeochemical feedbacks to the climate system: Changes in greenhouse gas sources and sinks

In a sensitivity study, we used the Lund-Potsdam-Jena Dynamic Global Vegetation Model (Sitch et al. 2003) to develop a simple, but robust regression model relating NPP to carbon storage in plants and soils. Using this model we estimated steady-state biomass simulated by BIOME4 in the control and 2 °C warming scenarios. Carbon storage in plants and soils calculated by BIOME4 roughly doubles in the Arctic in the 2 °C warming experiments

compared to the present-day simulation, with a total potential increase of ca. 600 Pg C in the robust mean and mean experiments, and over 1000 Pg C in the 90th percentile "warm" scenario. The increase in forest area and productivity is mainly responsible for these large changes in carbon storage, though shifts to taller and denser tundra types will also sequester more carbon both above and below ground.

The time lag associated with the development of forests makes it unlikely that the increase in carbon storage in the Arctic would be fully realized over the next century. Indeed, recent studies that synthesize widespread measurements indicate that Arctic tundra ecosystems have recently become a net source of carbon to the atmosphere (Oechel et al. 1993). Not included in this study is the possibility of large releases of carbon from frozen tundra peatlands, where typically a small percent of annual vegetation productivity is sequestered into permafrost. Expected warmer year-round temperatures could induce widespread thawing of frozen soils, which could indeed be responsible for large releases of CO_2 from the Arctic landscape on the short term (Christensen et al. 1999; Pastor et al. 2003; Frey and Smith 2005). On the time scale of several centuries, however, development of forests and forest soils in areas that are currently occupied by tundra could significantly increase the amount of carbon sequestered in the Arctic.

4 Discussion and conclusions

This paper has had three main objectives: (1) to provide an estimate of the time-range within which global mean temperature might increase to 2 °C above its pre-industrial level, (2) to describe the possible changes in Arctic climate that will accompany a 2 °C global temperature increase, and (3) to illustrate the effect that a 2 °C global warming could have on Arctic vegetation cover. As this involves projections into the future – with its associated uncertainties about emissions of GHGs and aerosols and their associated atmospheric concentrations – the study makes use of results from seven coupled ocean-atmosphere GCMs forced with four emission/concentration scenarios. Differences between GCMs and between forcing scenarios result in a range of dates at which global mean temperature anomaly is predicted to reach +2 °C: between 2026 and 2060, with a median date of 2043.

The geography of the Arctic (land-sea distribution) and snow/ice albedo feedbacks, along with changes in cloud and ocean heat transport, lead to an amplified regional warming over the Arctic that ranges from between 3.2 and 6.6 °C for a global change of +2 °C. In each of the GCMs that were evaluated, the amplification is similar for fast and slow warming scenarios, so changes in the Arctic predicted by a single model will be comparable regardless of when a global change of +2 °C occurs. However, a faster global warming will necessarily produce more rapid warming in the Arctic. The Arctic temperature change amplification means that these rates of warming are likely to be between 0.45–0.75 °C/decade, and possibly even as large as 1.55 °C/decade.

These results are derived from transient simulations of climate change driven by progressive forcing of climate by GHGs and aerosols through the 20th and 21st century, and therefore represent a climate system that has not reached equilibrium. It is important to realize that the ultimate climate changes in the Arctic, should global temperature change be stabilized near +2 °C, may be quite different, particularly as the oceans equilibrate with the atmosphere and interact with sea-ice. However, there are too few long-duration GCM simulations to equilibrium after stabilization (Mitchell et al. 2000; Dai et al. 2001) to address this rigorously.

Warming over the Arctic is largest in winter (4–10 °C, median of 6 °C) and least in summer (1.5–3.5 °C, median of 2.6 °C). These area-averaged changes mask important regional patterns of change. Winter warming is largest in the Arctic Ocean, and varies from model to model according to model-specific changes in sea-ice, while summer warming is largest over land. Thus, the contrast between winter and summer is smaller over land than over the Arctic Ocean. Most models show relatively little warming or even localized cooling over the North Atlantic and Greenland Sea, which is related to reduced strength and/or reorganization of the North Atlantic thermohaline circulation.

All models show increases in Arctic-wide precipitation, but spatial patterns of change vary considerably between models, with some localized decreases in precipitation. These increases in precipitation will, however, be accompanied by changes in the character of precipitation. Although information on the proportion of precipitation that falls as snow was not available for these GCMs, the increased warming implies that a higher fraction of precipitation will fall as rain; currently most summer precipitation, except in the central Arctic Ocean, falls as rain (Clark et al. 1996). For each season, we therefore expect the proportion of the Arctic that receives wet precipitation to increase, but for snow mass to increase where it remains cold enough for snow. In a study that used a similar set of 21st century climate simulations over the Arctic, Meleshko et al. (2004), showed that March snowmass increased, in line with greater winter precipitation, and that May snowmass decreased, due to increased rates of melting and reduced solid precipitation in spring. These changes have the potential to alter the hydrological regimes of river basins in the Arctic, with earlier spring snowmelt and more direct runoff earlier in the summer, and increased number of rain-on-snow events contributing to faster snowmelt and more intense flash floods (ACIA 2004).

Evaluations of GCM sea ice distributions in control simulations, (for example, Hu et al. 2004) have shown that all models have difficulty replicating the observed distributions and thicknesses, and that the magnitude of the snow/ice-albedo feedback effect (and hence regional temperature change) can be sensitive to the distribution and thickness of ice in a model's control climatology. Similarly, GCMs vary widely in their ability to replicate the average behavior and variability of mechanisms influencing Arctic climate (such as the North Atlantic Oscillation and the Atlantic thermohaline circulation). This is reflected in the wide range of predicted climate changes for the Arctic between the GCMs studied here. Where there is a consensus between GCMs one can be more confident in the robustness of the results of this analysis. For example, all GCMs exhibit greater warming in the Arctic than the global mean warming, so we can be confident in this result. However, the size of Arctic warming relative to global warming varies widely between models and we have little or no basis on which to judge whether one model is "better" than others. Therefore, calculation of a "mean Arctic temperature change" across all models has little meaning; rather, the range in predicted changes provides us with some bounds on the likely temperature changes, but also an indication of the rather large uncertainties in the current generation of GCM simulations of Arctic climate change.

A further source of uncertainty in this study arises from the analysis of only a single realization of each GCM-scenario combination. Single simulations make it difficult to quantify the relative contributions of natural variability and GHG forcing in the change in the Arctic at a time of 2 °C global warming. Indeed, it is possible that multiple simulations with the same GCM may produce differences as large as the differences between the models studied here. More robust results could be achieved through analysis of ensembles of simulations, but this was not possible with data available from the IPCC Data Distribution Centre. However, by analyzing the results for four difference GHG scenarios, and comparing between simulations at the time when the global temperature anomaly reaches 2 °C, some idea of

the relative importance of within and between-model differences can be gained. In general, differences between models are greater than difference within models, suggesting that the range of temperature and precipitation changes is mostly related to GCM choice rather than within-model variability. However, within-model variability does play a secondary role in the variability of results presented here. This is in agreement with the results of Raisanen (2001a), who estimated for the CMIP models that internal model "noise" accounted for only 10% (temperature) and 30% (precipitation) of the between-model variation in climate change at the time CO_2 doubling.

The results presented here provide strong evidence that high-latitude ecosystems are sensitive to climate change due to increases in greenhouse gas concentrations. Paleodata-model comparisons with the same classification scheme and vegetation model give confidence in the ability of the modeling procedure to simulate the potential consequences of climate change on vegetation in the Arctic. The four global 2 °C warming experiments performed here all show dramatic changes in the landscape of the Arctic. Modeled forest extent increases in the Arctic on the order of $3 \times 106\ km_2$ or 55% with a corresponding 42% reduction in tundra area. Tundra types generally also shift north with the largest reductions in the prostrate dwarf-shrub tundra, where nearly 60% of habitat is lost. Modeled shifts in the potential northern limit of trees reach up to 400 km from the present tree line.

Biophysical implications of this vegetation change include reduced albedo, which would have important feedbacks to the atmosphere, and changes in hydrological regimes because of increased snow retention. The increase in forest area in the Arctic would eventually be responsible for a large increase in carbon storage, though this could be offset by the thawing and oxidation of currently frozen organic soils. The changes in Arctic vegetation simulated here would almost certainly have ramifications for biodiversity, effects on animal populations and human activities.

While the Arctic can be considered an extreme example (at least in terms of temperature change), we have shown that the regional impacts of a relatively low global temperature stabilization target can remain significant. Indeed, the changes in climate, hydrology, and vegetation and associated ecosystem distributions that we describe, coupled with changes in sea ice in reported by Comiso and co-authors (2003, 2005) are likely to be catastrophic to for the wider Arctic system and its communities (ACIA 2004).

Further work should include vegetation-atmosphere coupling, allowing for the different physical properties in different vegetation types (including the major differences among the tundra types). The tundra classification used here could provide an initial basis for quantifying these properties. Additional studies should also address the transient nature of the climate change, accounting for development of vegetation, pedogenesis and permafrost dynamics.

Acknowledgements This work was supported by the World Wildlife Fund Arctic Programme. JOK received additional support from a Marie Curie Fellowship from the European Commission and was hosted by the Joint Research Centre. We are especially grateful to Lynn Rosentrater for her comments and editorial assistance. We acknowledge the NASA SRB project for insolation data, and Joel Daroussin, Arwyn Jones and Bob Jones of the European Soil Bureau for assistance on gathering soils data. We thank Terry Chapin, Torben Christensen and seven anonymous reviewers for their thorough, helpful comments, which improved this manuscript.

References

ACIA (2004) Impacts of a warming arctic: arctic climate impact assessment. Cambridge University Press, Cambridge, 146 pp

Allen MR, Ingram WJ (2002) Constraints on future changes in climate and the hydrologic cycle. Nature 419:224–232
Bonan GB, Chapin FS, Thompson SL (1995) Boreal forest and tundra ecosystems as components of the climate system. Climatic Change 29:145–167
Callaghan TV, Björn LO, Chapin FS, Chernov Y, Christensen TR, Huntley B, Ims R, Johansson M, Riedlinger DJ, Jonasson S, Matveyeva NV, Oechel WC, Panikov N, Shaver G (2005) Arctic Tundra and Polar Desert Ecosystems. Arctic Climate Impacts Assessment: Scientific Report, 243–352
Callaghan TV, Bjorn LO, Chernov Y, Chapin T, Christensen TR, Huntley B, Ims RA, Johansson M, Jolly D, Jonasson S, Matveyeva N, Panikov N, Oechel W, Shaver G, Schaphoff S, Sitch S (2004) Effects of changes in climate on landscape and regional processes, and feedbacks to the climate system. Ambio 33:459–468
CAVM-Team (2003) Circumpolar Arctic vegetation map, scale 1:7,500,000, conservation of arctic flora and fauna. Map No. 1 ed., U.S. Fish and Wildlife Service. http://www.geobotany.uaf.edu/cavm
Chapin FS, Eugster W, McFadden JP, Lynch AH, Walker DA (2000) Summer differences among Arctic ecosystems in regional climate forcing. J Climate 13:2002–2010
Chapin FSI, Bret-Harte MS, Hobbie SE, Zhong HL (1995) Plant functional types as predictors of transient responses of Arctic vegetation to global change. J Veg Sci 7:347–358
Christensen TR (1999) Potential and actual trace gas fluxes in Arctic terrestrial ecosystems. Polar Res 18:199–206
Christensen TR, Jonasson S, Callaghan TV, Havstrom M (1999) On the potential CO_2 release from tundra soils in a changing climate. Appl Soil Ecol 11:127–134
Christensen TR, Prentice IC, Kaplan J, Haxeltine A, Sitch S (1996) Methane flux from northern wetlands and tundra: an ecosystem source modelling approach. Tellus B 48:652–661
Clark MP, Serreze MC, Barry RG (1996) Characteristics of Arctic Ocean climate based on COADS data, 1980–1993. Geophys Res Lett 23:1953–1956
Comiso JC (2005) Impact Studies of a 2 °C global warming on the arctic Sea ice cover. evidence and implications of dangerous climate change in the Arctic, Rosentrater LD Ed., WWF, Oslo, 43–55
Comiso JC, Yang JY, Honjo S, Krishfield RA (2003) Detection of change in the Arctic using satellite and in situ data. J Geophys Res Oceans 108:art. no.-3384
Cramer W, Bondeau A, Woodward FI, Prentice C, Betts RA, Brovkin V, Cox PM, Fisher V, Foley JA, Friend AD, Kucharik C, Lomas MR, Ramankutty N, Sitch S, Smith B, White A, Young-Molling C (2001) Global response of terrestrial ecosystem structure and function to CO_2 and climate change: results from six dynamic global vegetation models. Glob Change Biol 7:357–374
Curry JA, Rossow WB, Randall D, Schramm JL (1996) Overview of Arctic cloud and radiation characteristics. J Climate 9:1731–1764
Dai AG, Wigley TML, Meehl GA, Washington WM (2001) Effects of stabilizing atmospheric CO_2 on global climate in the next two centuries. Geophys Res Lett 28:4511–4514
de Noblet NI, Prentice IC, Joussaume S, Texier D, Botta A, Haxeltine A (1996) Possible role of atmosphere-biosphere interactions in triggering the last glaciation. Geophys Res Lett 23:3191–3194
Delworth TL, Stouffer RJ, Dixon KW, Spelman MJ, Knutson TR, Broccoli AJ, Kushner PJ, Wetherald RT (2002) Review of simulations of climate variability and change with the GFDL R30 coupled climate model. Clim Dynam 19:555–574
FAO: Digital Soil Map of the World and Derived Soil Properties
Flato GM (2004) Sea-ice and its response to CO_2 focing as simulated by global climate models. Clim Dynam 23:229–241
Flato GM, Boer GJ (2001) Warming asymmetry in climate change simulations. Geophys Res Lett 28:195–198
Foley JA, Kutzbach JE, Coe MT, Levis S (1994) Feedbacks between climate and boreal forests during the Holocene epoch. Nature 371:52–54
Frey KE, Smith LC (2005) Amplified carbon release from vast West Siberian peatlands by 2100. Geophys Res Lett 32
Gordon C, Cooper C, Senior CA, Banks H, Gregory JM, Johns TC, Mitchell JFB, Wood RA (2000) The simulation of SST, sea ice extents and ocean heat transports in a version of the Hadley Centre coupled model without flux adjustments. Clim Dynam 16:147–168
Hansen JE (2005) A slippery slope: How much global warming constitutes "dangerous anthropogenic interference"? Climatic Change 68:269–279
Harrison SP, Jolly D, Laarif F, Abe-Ouchi A, Dong B, Herterich K, Hewitt C, Joussaume S, Kutzbach JE, Mitchell J, de Noblet N, Valdes P (1998) Intercomparison of simulated global vegetation distributions in response to 6 kyr BP orbital forcing. J Climate 11:2721–2742

Haxeltine A, Prentice IC (1996a) BIOME3: an equilibrium terrestrial biosphere model based on ecophysiological constraints, resource availability, and competition among plant functional types. Global Biogeochem Cy 10:693–709
Haxeltine A, Prentice IC (1996b) A general model for the light-use efficiency of primary production. Funct Ecol 10:551–561
Haxeltine A, Prentice IC, Creswell ID (1996) A coupled carbon and water flux model to predict vegetation structure. J Veg Sci 7:651–666
Hennessy KJ, cited (2004) Climate change output. http://www.dar.csiro.au/publications/hennessy_1998a.html
Holland MM, Bitz CM (2003) Polar amplification of climate change in coupled models. Clim Dynam 21:221–232
Hu ZZ, Kuzmina SI, Bengtsson L, Holland DM (2004) Sea-ice change and its connection with climate change in the Arctic in CMIP2 simulations. J Geophys Res-Atmos 109:art. no.-D10106
Ingram WJ, Wilson CA, Mitchell JFB (1989) Modeling climate change - an assessment of sea ice and surface albedo feedbacks. J Geophys Res-Atmos 94:8609–8622
IPCC (1995) Climate change 1995: the science of climate change. Cambridge University Press, Cambridge, 453 pp
IPCC (2001a) Climate change 2001: impacts, adaptation, and vulnerability. Contribution of Working Group II to the third assessment report of the Intergovernmental Panel on Climate Change. Cambridge University Press, Cambridge, UK New York, 1032 pp
IPCC (2001b) Climate change 2001: the scientific basis. Contribution of Working Group I to the third assessment report of the Intergovernmental Panel on Climate Change. Cambridge University Press, Cambridge, 881 pp
Johannessen OM, Bengtsson L, Miles MW, Kuzmina SI, Semenov VA, Alekseev GV, Nagurnyi AP, Zakharov VF, Bobylev LP, Pettersson LH, Hasselmann K, Cattle HP (2004) Arctic climate change: observed and modelled temperature and sea-ice variability. Tellus A 56:328–341
Jolly D, Haxeltine A (1997) Effect of low glacial atmospheric CO_2 on tropical African montane vegetation. Science 276:786–788
Jones PD, New M, Parker DE, Martin S, Rigor IG (1999) Surface air temperature and its changes over the past 150 years. Rev Geophys 37:173–199
Joos F, Prentice IC, Sitch S, Meyer R, Hooss G, Plattner G-K, Gerber S, Hasselmann K (2001) Global warming feedbacks on terrestrial carbon uptake under the Intergovernmental Panel on Climate Change (IPCC) emission scenarios. Global Biogeochem Cy 15:891–907
JRC (2003) GLC2000: global land cover map for the year 2000. European Commission Joint Research Centre. http://www.gvm.jrc.it/glc2000
Kaplan JO (2001) Geophysical applications of vegetation modeling, Ph.D. thesis, department of ecology. Lund University, 132 pp
Kaplan JO (2002) Wetlands at the Last glacial maximum: distribution and methane emissions. Geophys Res Lett 29:3.1–3.4
Kaplan JO, Prentice IC, Buchmann N (2002) The stable carbon isotope composition of the terrestrial biosphere: modeling at scales from the leaf to the globe. Global Biogeochem Cy 15:8.1–8.11
Kaplan JO, Bigelow NH, Bartlein PJ, Christensen TR, Cramer W, Harrison SP, Matveyeva NV, McGuire AD, Murray DF, Prentice IC, Razzhivin VY, Smith B, Walker DA, Anderson PM, Andreev AA, Brubaker LB, Edwards ME, Lozhkin AV (2003) Climate change and Arctic ecosystems: 2. Modeling, paleodata-model comparisons, and future projections. J Geophys Res-Atmos 108:12.11–12.17
Kling GW, Kipphut GW, Miller MC (1991) Arctic lakes and streams as gas conduits to the atmosphere - implications for tundra carbon budgets. science 251:298–301
Meleshko VP (2004) Changes in Arctic snow mass in the 21st century. Russian Meteorology and Hydrology, 2004
Mitchell JFB, Johns TC, Ingram WJ, Lowe JA (2000) The effect of stabilising atmospheric carbon dioxide concentrations on global and regional climate change. Geophys Res Lett 27:2977–2980
New M, Lister D, Hulme M, Makin I (2002) A high-resolution data set of surface climate over global land areas. Climate Res 21:1–25
New MG (2005) Arctic climate change with a 2 °C global warming. In: Rosentrater LD (ed) Evidence and implications of dangerous climate change in the Arctic. WWF, Oslo, 1–15
Nozawa T, Emori S, Numaguti A, Yoko Tsushima, Takemura T, Nakajima T, Abe-Ouchi A, Kimoto M (2001) Projections of future climate change in the 21st century simulated by the CCSR/NIES CGCM under the IPCC SRES scenarios. In: Matsuno T, Kida H (eds) Present and future of modeling global environmental change: Toward integrated modeling. TERRAPUB, pp 15–28
Oechel WC, Hastings ST, Vourlitis G, Jenkins M, Riechers G, Grulke N (1993) Recent change of Arctic tundra ecosystems from a net carbon dioxide sink to a source. Nature 361:520–523

Pastor J, Solin J, Bridgham SD, Updegraff K, Harth C, Weishampel P, Dewey B (2003) Global warming and the export of dissolved organic carbon from boreal peatlands. Oikos 100:380–386

Polyakov IV, Bekryaev RV, Alekseev GV, Bhatt US, Colony RL, Johnson MA, Maskshtas AP, Walsh D (2003) Variability and trends of air temperature and pressure in the maritime Arctic, 1875–2000. J Climate 16:2067–2077

Polyakov IV, Alekseev GV, Bekryaev RV, Bhatt U, Colony RL, Johnson MA, Karklin VP, Makshtas AP, Walsh D, Yulin AV (2002) Observationally based assessment of polar amplification of global warming. Geophys Res Lett 29:art. no. 1878

Prentice IC, Cramer W, Harrison SP, Leemans R, Monserud RA, Solomon AM (1992) A global biome model based on plant physiology and dominance, soil properties and climate. J Biogeogr. 19:117–134

Przybylak R (2000) Temporal and spatial variation of surface air temperature over the period of instrumental observations in the Arctic. Int J Climatol 20:587–614

Raisanen J (2001a) CO_2-induced climate change in CMIP2 experiments: quantification of agreement and role of internal variability. J Climate 14:2088–2104

Raisanen J (2001b) CO_2-induced climate change in the Arctic area in the CMIP2 experiments. SWECLIM Newsletter 11:23–28

Rauthe M, Paeth H (2004) Relative importance of northern hemisphere circulation modes in predicting regional climate change. J Climate 17:4180–4189

Reynolds CA, Jackson TJ, Rawls WJ (1999) Estimating available water content by linking the FAO soil map of the World with global soil profile databases and pedo-transfer functions. AGU Spring Meeting, Boston, MA, American Geophysical Union

Roeckner E, Arpe K, Bengtsson L, Christoph M, Claussen M, Dümenil L, Esch M, Giorgetta M, Schlese U, Schulzweida U (1996) The atmospheric general circulation model ECHAM-4: model description and simulation of present-day climate. Max-Planck Institute for Meteorology Report No.218

Serreze MC, Walsh JE, Chapin FS, Osterkamp T, Dyurgerov M, Romanovsky V, Oechel WC, Morison J, Zhang T, Barry RG (2000) Observational evidence of recent change in the northern high- latitude environment. Climatic Change 46:159–207

Sitch S, Smith B, Prentice IC, Arneth A, Bondeau A, Cramer W, Kaplan JO, Levis S, Lucht W, Sykes MT, Thonicke K, Venevsky S (2003) Evaluation of ecosystem dynamics, plant geography and terrestrial carbon cycling in the LPJ dynamic global vegetation model. Glob Change Biol 9:161–185

VEMAP (1995) Vegetation/ecosystem modeling and analysis project: comparing biogeography and biogeochemistry models in a continental-scale study of terrestrial ecosystem responses to climate-change and CO_2 doubling. Global Biogeochem Cy 9:407–437

Walker DA, Raynolds MK, Daniels FJA, Einarsson E, Elvebakk A, Gould WA, Katenin AE, Kholod SS, Markon CJ, Melnikov ES, Moskalenko NG, Talbot SS, Yurtsev BA, CAVM-Team (2005) The Circumpolar Arctic vegetation map. J Veg Sci 16:267–282